FLOW PAST A CURVED PIPE IN DIFFERENT IN-LINE CONFIGURATIONS UNDERGOING FORCED TRANSVERSE OSCILLATIONS

A. de Vecchi, S.J. Sherwin, J.M.R Graham
Department of Aeronautics, Imperial College London, UK

ABSTRACT

Three-dimensional numerical simulations using a spectral/hp element Navier-Stokes solver have been preformed on a curved cylinder forced to transversely vibrate at a Reynolds number of 100*. The configurations investigated are based on a circular cylinder whose centre-line is a quarter of a ring with a radius of curvature close to the limit value for real flexible riser pipes. A sinusoidal translation and an oscillatory roll about the bottom end of the quarter of a ring have been imposed to the body: the input frequency and amplitude have been varied inside and outside of the two-dimensional lock-in region for a straight circular cylinder at the same Reynolds number. The energy transfer mechanism has also been analysed to provide indications of which flow states are likely to occur in free vibration.*

1. INTRODUCTION

The complexity of the wake past curved riser pipes poses a challenging problem to the offshore industry, as the increasing need to exploit deep-water reservoirs has highlighted the lack of a complete insight into the Vortex-Induced Vibration (VIV) dynamic on such long structures. Among the first researchers who investigated the vortex shedding past curved cylinders at low Reynolds numbers, Takamoto and Izumi [1981] reported on the stable arrangement of vortex rings developed in experiments behind an axisymmetric ring. Leweke and Provansal [1995] studied the flow past a ring at sufficiently large aspect ratios (ring perimeter/cross section diameter > 30) that allow to approximate the flow patterns of a straight cylinder with periodic boundary conditions, hence discarding the influence of end effects; with smooth initial conditions parallel shedding was found to be dominant. Their results compare favourably with the numerical simulations behind a quarter of ring performed by Miliou et al. [2003] at $Re = 100$: in this case as well in-phase parallel shedding was observed when the flow was directed normal to the plane of curvature.

Miliou et al. [2007] investigated the same geometries in the case of a constant inflow parallel to the plane of curvature of the quarter ring at $Re = 100$ and $Re = 500$: only one dominant shedding frequency was found for the whole cylinder's span, with the vortex shedding in the upper part of the ring driving the one in the lower end. The wake exhibited a 2S mode of shedding, with straight cores, and a gradual phase shift was observed along the span of the cylinder as a result of curvature. However, in the reverse configuration no vortex shedding was detected and the near wake reached a steady state at both Reynolds numbers, achieving a drag reduction of 12%. Miliou et al. related the completely different wake features to the the generation of additional component of streamwise and vertical vorticity along the body span.

These results can be compared with the analysis of Darekar and Sherwin [2001] on bodies with a wavy leading edge. The authors observed a variation in the wake width along the span of the wavy cylinder and different flow regimes could be identified depending on the type of waviness: the so called regime III A was found to suppress vortex shedding with a drag reduction of 16%, leading to a symmetric wake with respect to the cylinder centreline in analogy with the concave configuration behaviour investigated by Miliou et al. [2007]. The experimental work of Bearman and Owen [1998], Bearman and Tombazis [1997] and Lam et al. [2004] confirms that a sufficiently high wave steepness stabilises the near wake in a time-independent state and results in drag reduction.

A useful approach to understand and eventually predict the occurrence of VIV is represented by forced vibration simulations. Williamson and Roshko [1988] studied the wake of a circular cylinder forced to move along a sinusoidal path in the range $300 < Re < 1000$ and identified three principal types of vortex patterns, named 2S, 2P and P+S. These results found confirmation in several studies of freely vibrating cylinders, such as Govardhan and Williamson [2000], Black-

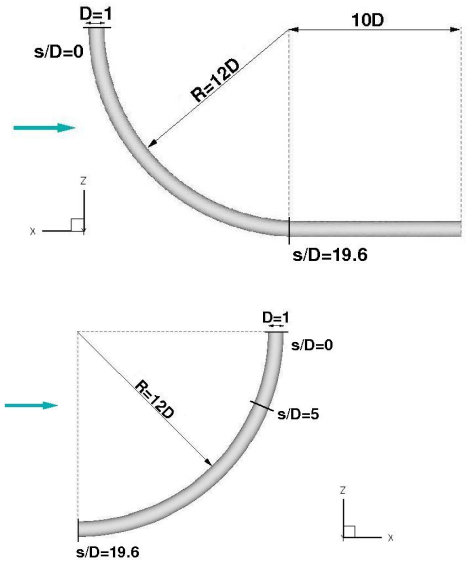

Figure 1: Convex configuration (a) and concave configuration (b); the arrows indicate the free-stream direction, whereas s/D is the non-dimensional arc-length.

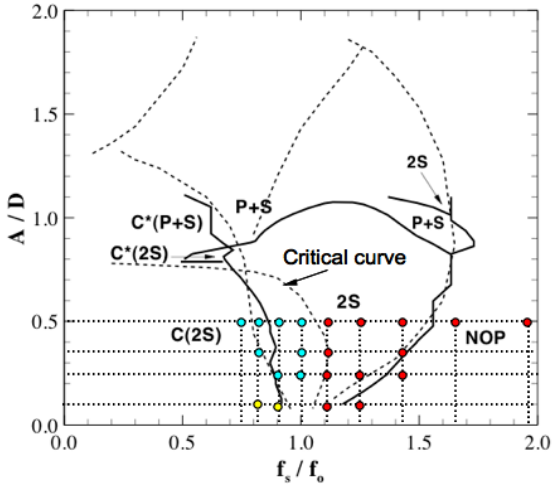

Figure 2: Map of vortex shedding modes for a tow-dimensional cylinder at $Re = 100$ [Willden et al., 2008] with the flow states analysed in the present simulations for the concave configuration case. Empty circles: wide-wake 2S. Filled circles: narrow-wake 2S.

burn et al. [2000] and Carberry et al. [2005]. In their two-dimensional simulations, Willden et al. [2008] established the lock-in boundary for vortex shedding of a cylinder forced to oscillate in the transverse direction at $Re = 100$. The flow states identified in this research will serve as a comparison basis for the present work, in which numerical simulations of forced oscillation cases at $Re = 100$ have been performed on the same geometries investigated in Miliou et al. [2003] and Miliou et al. [2007]: these conditions are meant to reproduce some of the features of a freely vibrating curved pipe under the simplified conditions provided by forced oscillations. Although the Reynolds number considered is several orders of magnitude lower than a realistic range for offshore applications, it allows to represent the fundamental features of the wake dynamics and to elucidate vortex shedding patterns that are likely to persist at higher Reynolds numbers.

2. NUMERICAL METHOD

The three-dimensional computations have been performed using a spectral/hp element Navier-Stokes solver developed by Sherwin and Karniadakis [1996], Karniadakis and Sherwin [2005]. The temporal discretisation is achieved by a stiffly stable splitting scheme which allows the primitive variables to be treated independently over a time step Δt. The solution at time t_{n+1} is obtained from the solution at t_n over three sub-steps. First, the non-linear term is treated explicitly, then a Poisson equation for the pressure is obtained by taking the divergence of the pressure term and by enforcing the incompressibility constraint. Finally the diffusive term is treated implicitly in the last sub-step. Overall one Poisson equation for the pressure and one Helmholtz equation for each of the velocity components are solved for every time step. Further details on the splitting scheme can be found in Karniadakis and Sherwin [2005].

3. PROBLEM DESCRIPTION

The two geometrical configurations considered are sketched in figure 1. As previously outlined, the inflow direction lies in the plane of curvature of the curved cylinder: according to whether the free-stream is directed towards the outside or the inside of the quarter ring, the geometries are labelled “convex” and “concave” (figure 1). A non-dimensional arc length, s/D, has been defined to identify the different spanwise locations: in both cases the end of the ring part is at $s/D = 19.6$ and the top section corresponds to $s/D = 0$.

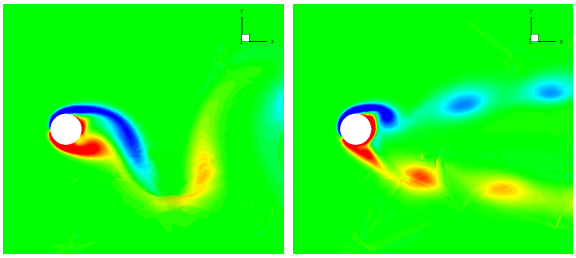

Figure 3: Vorticity component ω_z at the top section of the concave configuration forced to translate with $A/D = 0.5$. *Left*: $f_s/f_o = 1.111$. *Right:* $f_s/f_o = 0.909$.

4. TRANSVERSE TRANSLATION OF THE CONCAVE CONFIGURATION

The input parameters chosen in this study are illustrated by the dots on the plot in figure 2: this map was obtained by Willden et al. [2008] with two-dimensional simulations of a circular cylinder at $Re = 100$. In all the flow states simulated the shedding mode appears to be 2S; however, when the ratio of the Strouhal frequency over the input oscillation frequency (f_s/f_o) passes the critical curve, two different sub-regimes can be identified.

For $f_s/f_o > 1$ the wake appears narrow and the shear layers are elongated and undergo a gradual contraction as the input frequency f_o is increased: this wake dynamics is illustrated in figure 3 and resembles the conventional 2S shedding for a two-dimensional cylinder. However, figure 3 shows that a change in the shedding mechanism occurs and a much wider wake is generated as the oscillation frequency approaches the Strouhal value: a higher concentration of span-wise vorticity in the base region results in the generation of a secondary vortex between the two shear layers, which now appear remarkably contracted (figure 4). It is suggested that this flow state could be a very weak form of P+S shedding, in which the second vortex in the pair is not strong enough to be released in the near wake and merges with the primary core after being formed.

As mentioned earlier, Miliou et al. [2007] found that the vortex shedding past the concave geometry is suppressed in the absence of motion: the present study shows that the wake instabilitiy is resumed by the forced oscillation and the resulting Von Karman street is formed by vortex cores bent according to the body's curvature, as shown in figure 4. The shedding resumption is associated to the different distribution of the velocity component generated along the cylinder's axis: figure 6*(top)* shows that the axial velocity gradient, measured 0.3 diameters downstream in the radial direction, sharply increases for $1 < s/D < 7$: this range corresponds approximately to the top half of the quarter ring and represents the part of the curved cylinder most susceptible to exhibit vortex shedding. The axial velocity gradient in the forced oscillations is not as strong as in the steady case and follows two different trends depending on the sub-regimes of shedding, with a transitional behaviour between the two 2S states for input frequencies equal to the Strouhal value.

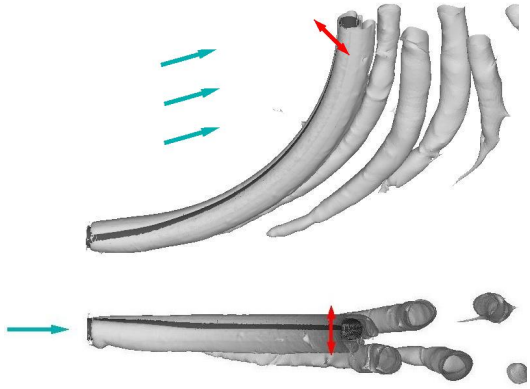

Figure 4: Concave configuration at $f_s/f_o = 0.91$, $A/D = 0.5$: isosurfaces at $\lambda_2 = -0.1$.

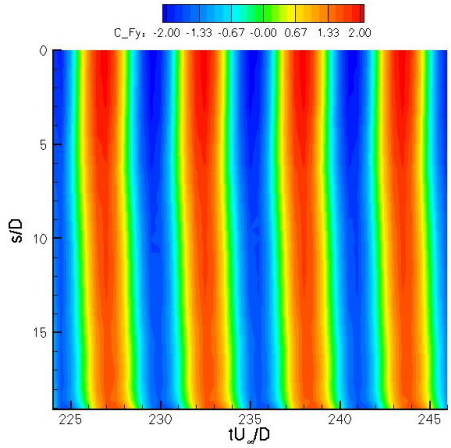

Figure 5: Concave configuration at $f_s/f_o = 0.91$, $A/D = 0.5$: spanwise variation of sectional lift coefficient

Figure 5 shows that the vortex shedding is in phase with the cylinder's motion in the case of a wide wake 2S. However, the net energy transfer associated to this sub-regime is negative for the whole body, meaning that the body is not

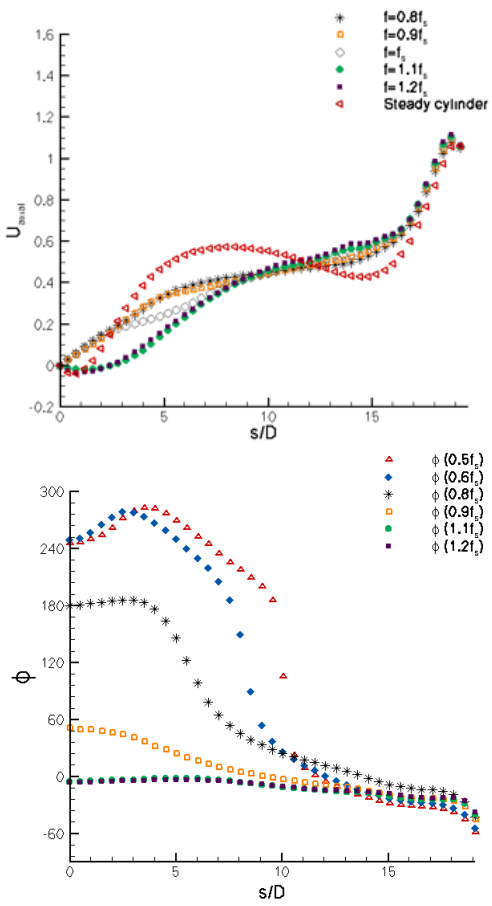

Figure 6: Transverse translation of the concave case. *Top*: time-averaged values of the axial velocity component at 0.3 diameters radially downstream. *Bottom*: phase angle variation along the span for different input frequencies.

excited by the flow and the phase angle is in the range $\phi[-180°, 0°]$(see figure 6*(bottom)* where $f_o = 1.1f_s$ and $f_o = 1.2f_s$ correspond to $f_s/f_o = 0.909$ and $f_s/f_o = 0.833$ respectively in the map in figure 2). The phase variation along the span depicted in figure 6*(bottom)* shows also that only the flow states associated to the narrow-wake 2S inside the lock-in region have a phase angle that lies in the positive energy transfer region $\phi[0°, 180°]$. These correspond to the cases with input frequencies $f_o = 0.8f_s$ and $f_o = 0.9f_s$.

5. FORCED OSCILLATION OF THE CONVEX CONFIGURATION

5.1. Transverse translation

For all the frequencies tested with amplitude $A/D = 0.5$, the vortex shedding past the convex

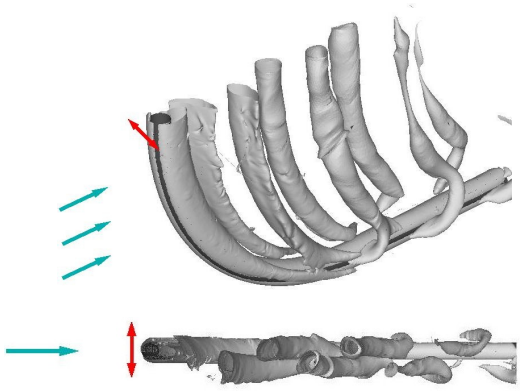

Figure 7: Convex configuration at $f_s/f_o = 1.111$, $A/D = 0.5$: isosurfaces at $\lambda_2 = -0.1$.

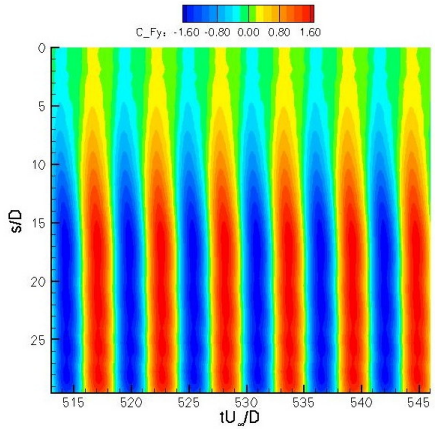

Figure 8: Convex configuration at $f_s/f_o = 1.111$, $A/D = 0.5$: spanwise variation of sectional lift coefficient. The horizontal extension is in the range $19.6 < s/D < 29.6$.

cylinder resembled to a more conventional form of 2S mode, exhibiting a narrow wake with curved cores (figure 7) and in-phase forces. However, unlike the concave case at the same amplitude, in this configuration the body could never be excited by the flow and the phase angle resulted negative, as shown in figure 9. This is related to the portion of the cylinder aligned to the inflow direction: the horizontal extension behaves in fact like a slender body and therefore act as a hydro-dynamic damper for the rest of the geometry (figure 8). To attenuate this effect the amplitude of motion was reduced to $0.25D$ and to $0.1D$: these flow states could indeed achieve a positive energy transfer in the top part, as shown by the phase diagram in figure 9.

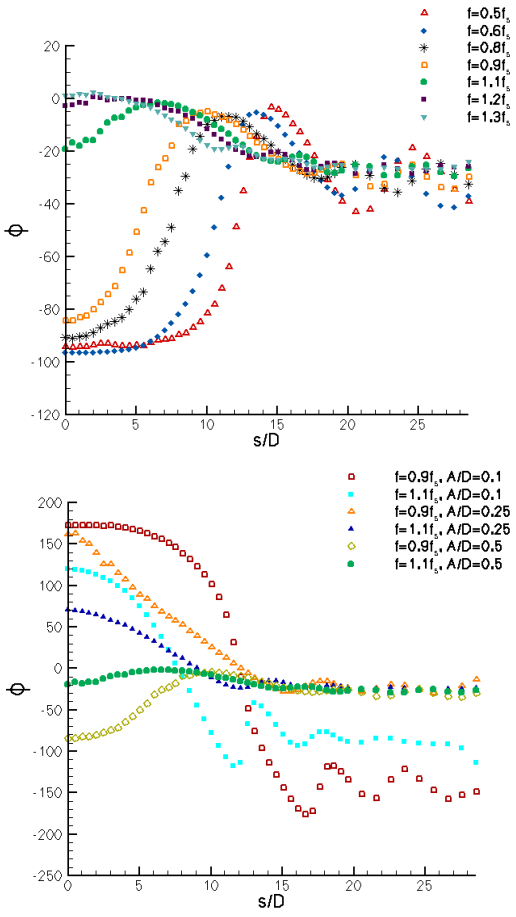

Figure 9: Convex configuration. Effect of frequency and amplitude variation on the phase angel at $A/D = 0.5$.

5.2. Transverse rotation about the horizontal extension axis

To reduce the damping effect in the convex configuration, an oscillatory roll about the horizontal extension axis has been imposed to the cylinder. This kind of oscillation presents similarities to the motion near the touch-down point in offshore structures. The maximum amplitude at the top section has been set to $0.5D$ in analogy with the previous cases. At an input frequency equal to $f_i = 0.9f_s$, the vortex cores are only slightly bent according to the cylinder's curvature and detach from the main vortex at different span-wise locations for every time instant. As shown in figure 11, they also exhibit a marked span-wise waviness, similar to the wake observed in free vibrations of a yawed cylinder at higher Reynolds numbers [Lucor and Karniadakis, 2003]. Unlike the forced translation cases, the main vortex is weaker and does not envelope the horizontal extension, which is now fixed. As expected, the outcome of this type of motion is a gradual phase shift towards the excitation region where $\phi[0°, 180°]$ and large "pockets" of positive excitation appear along the cylinder's span (figure 10.

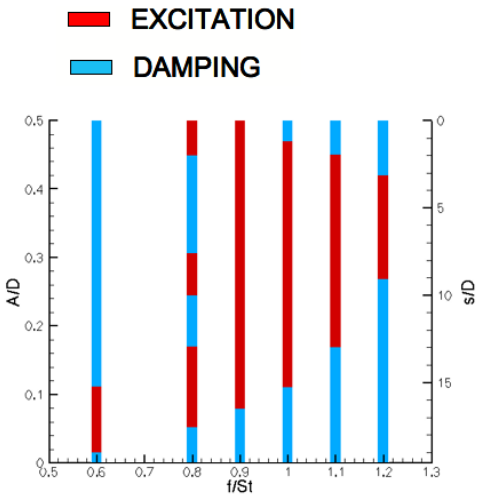

Figure 10: Excitation and damping regions along the span of the convex configuration in forced rotation about the horizontal extension axis.

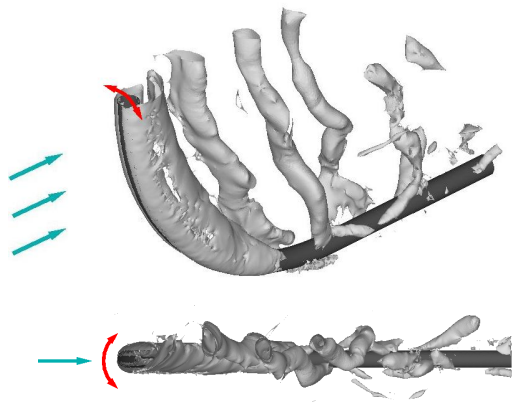

Figure 11: Wake topology for the flow past the convex configuration in transverse rotation at $f_i = 0.9f_s$ visualised through isosurfaces at $\lambda_2 = -0.1$.

6. CONCLUSION

Numerical simulations of forced oscillations have been performed on two curved geometries in the laminar shedding regime. In particular, we have addressed the question of the role played in the wake dynamics by the curvature of the stagnation face and we have investigated the energy transfer mechanism to identify the flow states that may

be associated to VIV. A parametric study, using amplitude and frequency of vibration as input parameters, was therefore undertaken. The concave case, which suppressed vortex shedding in the fixed cylinder case, presented a primary instability in the wake when forced to oscillate in the cross-stream direction. Vortex shedding resumed and two different 2S sub-regimes, respectively characterised by a wide and a narrow wake topology, were identified by varying the input frequency. For oscillation frequencies below the Strouhal value for a fixed two-dimensional cylinder (right of the critical curve in the map produced by Willden et al. [2008]) the narrow-wake 2S mode was found to be predominant, while for frequencies above the Strouhal value a wide-wake 2S mode was observed. In the concave configuration, only the narrow-wake 2S mode presented a positive energy transfer. The convex cylinder exhibited a different wake dynamics, as the horizontal extension provided a strong hydro-dynamic damping, preventing the structure to reach positive values of energy transfer. To achieve flow excitation in this case, two approaches have been attempted. A reduction in the oscillation amplitude was found to reduce the damping effect until the energy transfer changed sing. Likewise, a transverse rotation about the the extension axis allowed to shift the phase angle to the positive excitation range ($\phi \in [0°, 180°]$). However, this rotatory motion radically changed the physics of the wake, resulting in a high distortion of the vortex cores and out-of-phase shedding.

7. REFERENCES

P.W. Bearman and J.C. Owen, 1998, Reduction of bluff-body drag and suppression of vortex shedding by the introduction of wavy separation lines. *Journal of Fluid and Structures*, **12**:123–130.

P.W. Bearman and N. Tombazis, 1997, A study of the three-dimesional aspects of vortex shedding from a bluff body with a mild geometric disturbance. *Journal of Fluid Mechanics*, **330**: 85–112.

H.M. Blackburn, R. Govardhan, and C.H.K. Williamson, 2000, A complimentary numerical and physical investigation of vortex-induced vibration. *Journal of Fluids and Structures*, **15**: 481–488.

J. Carberry, J. Sheridan, and D. Rockwell, 2005, Controlled oscillations of a cylinder: forces and wake modes. *Journal of Fluid Mechanics*, **538**: 31–69.

R. M. Darekar and S. J. Sherwin, 2001, Flow past a square-section cylinder with a wavy stagnation face. *Journal of Fluid Mechanics*, **426**:263–295.

R. Govardhan and C.H.K. Williamson, 2000, Modes of vortex formation and frequency response of a freely vibrating cylinder. *Journal of Fluid Mechanics*, **420**:85–130.

G. E. Karniadakis and S. J. Sherwin, 2005, *Spectral/hp Element Methods for CFD*. Oxford University Press.

K. Lam, F.H. Wang, and So R.M.C, 2004, Three-dimensional nature of vortices in the near wake of a wavy cylinder. *Journal of Fluids and Structures*, **19**:815–833.

T. Leweke and M. Provansal, 1995, The flow behind rings - bluff-body wakes without end effects. *Journal of Fluid Mechanics*, **288**:265–310.

D. Lucor and G.E. Karniadakis, 2003, Effects of oblique inflow in vortex-induced vibrations. *Flow, turbulence and combustion*, **71**:375–389.

A. Miliou, S.J. Sherwin, and J.M.R. Graham, 2003, Fluid dynamic loading on curved riser pipes. *ASME Journal of Offshore Mechanics and Arctic Engineering*, **125**:176–182.

A. Miliou, A. de Vecchi, S. J. Sherwin, and J. M. R. Graham, 2007, Wake dynamics of external flow past a curved cylinder with the free-stream aligned to the plane of curvature. *Journal of Fluid Mechanics*, **592**:89–115.

S.J. Sherwin and G.E. Karniadakis, 1996, Tetrahedral hp finite elements: algorithms and flow simulations. *Journal of Computational Physics*, **124**:14–45.

M. Takamoto and K. Izumi, 1988, Experimental observation of stable arrangement of vortex rings. *Physics of Fluids*, **24**:1582–1583.

R.H.J Willden, R.J. McSherry, and J.M.R. Graham, 2008, Prescribed cross-stream oscillations of a circular cylinder at laminar and early turbulent reynolds numbers. *Proceedings of the Fifth Bluff Bodies and Vortex-Induced Vibration Conference, Brazil.*

C.H.K. Williamson and A. Roshko, 1988, Vortex formation in the near wake of an oscillating cylinder. *Journal of Fluid and Structures*, **2**:355–381.